An Improved Limit Equilibrium Method for Stability Analysis of Unsaturated Soil Slopes

Kai Liu

Department of Civil and Environmental Engineering, The Hong Kong Polytechnic University, Kowloon, Hong Kong, China; College of Civil and Transportation Engineering, Shenzhen University, Shenzhen, China

Weihang Ouyang & Si-wei Liu

Department of Civil and Environmental Engineering, The Hong Kong Polytechnic University, Kowloon, Hong Kong, China

Jian-hua Yin

Department of Civil and Environmental Engineering, The Hong Kong Polytechnic University, Kowloon, Hong Kong, China; College of Civil and Transportation Engineering, Shenzhen University, Shenzhen, China

doi: https://doi.org/10.21467/proceedings.7.7.20

ABSTRACT

Unsaturated soil is widely distributed around the world but less considered in design due to the absence of a convenient analysis method in practice. The Morgenstern-Price (MP) method incorporating the extended Mohr–Coulomb shear strength equation provides a reliable approach to evaluating slope stability in such conditions. However, this method is time-consuming due to the need for a tedious trial-and-error process in determining the scaling factor, which involves complex iterations during each trial. Furthermore, since the relatively complicated nature of unsaturated soil, a dense slice division is necessary to obtain reliable results, making the analysis even more cumbersome. In this paper, an improved MP method for unsaturated soil slope stability analysis is presented, which eliminates the need for a dense slice mesh by employing only a few strategically placed Gauss points along the slip surface. Moreover, the trial-and-error process for determining the scaling factor with the corresponding complex iterations is replaced by an efficient search algorithm with a more concise iteration process, resulting in a more convenient implementation of the proposed method. Extensive examples are provided to validate the effectiveness of the proposed improved MP method, indicating its potential as an accurate and efficient analysis method for unsaturated soil slopes in practical application and relative study involving repetitive analyses.

1 INTRODUCTION

Unsaturated soil slopes present a critical concern in geotechnical engineering due to the significant reduction in soil shear strength caused by water infiltration (Cai & Ugai 2004). Such strength reduction can cause severe failures in both natural and man-made slopes, especially for those in reservoir areas, such as more than 60 landslides occurred in the Three Gorges Reservoir region since 2003 (Xiong et al. 2019). The primary triggers for these landslides are repeated water infiltration due to rainfall and fluctuating reservoir water levels, leading to significant damage to both human life and engineering structures. Although analyzing slope stability based on saturated soil mechanics might appear as an approach to prevent such catastrophic events, it sometimes results in excessively conservative and inefficient design outcomes, imposing substantial construction costs for large-scale geotechnical projects (Houston 2019). Thus, the feature of unsaturated soil slope must be appropriately evaluated for a safe and economical design result. In practice, however, slope stability analyses commonly neglect suction effects, not only due to a lack of suitable analysis methods but also because conservative design practices intentionally omit these beneficial effects to ensure safety margins.

Various methods have been developed for slope stability analysis over the past few decades, including limit analysis method (LAM) (Sun et al. 2019), finite element method (FEM) (Griffiths & Lu 2005), and limit equilibrium method (LEM) (Duncan 1996; Ouyang et al. 2022). The LAM is usually used in simple geotechnical problems but less suitable for complicated geological conditions in engineering practice. For

Proceedings DOI: 10.21467/proceedings.7.7; Series: AIJR Proceedings; ISSN: 2582-3922; ISBN: 978-81-989164-3-3

more general slope stability analysis methods, the FEM has been employed to evaluate the slope stability by incorporating the strength reduction technique. This method is robust; however, it requires solid knowledge of constitutive models, linear and nonlinear failure criteria, and plasticity flow rules for determining critical slip surfaces. In addition, the effort and cost of FEM are sometimes unbearable in design practice. Consequently, the LEM is still the predominant slope stability analysis method in current design practice and recommended by various specifications.

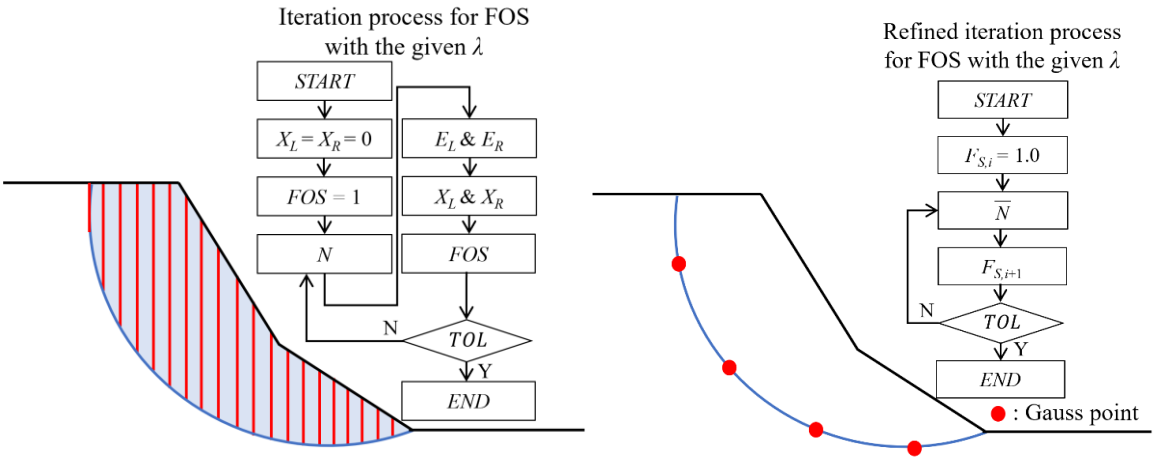

(a) The traditional MP method (b) Present study

Figure 1: Comparison between the traditional MP method and the present study

In the conventional LEM, the potential sliding soil mass is required to be discretized as vertical slices. The factor of safety (FOS) is calculated based on the force and moment equilibrium of the potential sliding soil mass. Different methods have been proposed based on various assumptions of interslice forces and satisfied conditions for force and moment equilibrium (Cheng & Lau 2014), including Bishop method, Morgenstern-Price (MP) method, Spencer method, Sarma method, and Janbu method. Among these methods, the MP method is the most widely used approach since it satisfies stricter equilibrium conditions. Subsequently, various shear strength equations, such as the extended Mohr–Coulomb shear strength equation (Fredlund et al. 1978), have been introduced in this method to extend it from only saturated/dry soil slopes to those unsaturated. However, this MP method is still less employed for the unsaturated slope stability analysis in design practices since it is relatively time-consuming and complicated in implementation.

In this study, an efficient numerical implementation of the LEM for stability analysis of unsaturated soil slopes is presented. An improved MP method proposed by Ouyang et al. (2022) for dry slopes is extended to evaluate the stability of unsaturated soil slopes, where the dense division of slice is replaced by the alignment of only several Gauss points. To improve the searching efficiency of the scaling factor, a linear search method is introduced to replace the best-fit method. Moreover, this paper firstly proposes a refined iteration process for the FOS with the given scaling factor (as shown in Fig. 1b), making the implementation process of the improved MP method for unsaturated slopes more convenient and efficient. To validate the robustness and efficiency of the proposed method, two benchmark examples are provided, including homogeneous and nonhomogeneous unsaturated soil slopes. Finally, one case study of unsaturated residual soil slope in Hong Kong is illustrated for future applications in engineering practice. It is believed that this improved MP method for unsaturated slopes will be a useful tool for investigating the unsaturated feature of slope stability in design practice.

2 THE IMPROVED MORGENSTERN-PRICE METHOD

2.1 The factors of safety F_m and F_f

In the traditional MP method, the slice division must be dense enough by increasing the slice number to achieve the reliable results. When the slice of width, b_i, trends to be infinitesimally small and the slice number, n, is infinite, the FOSs when considering the moment equilibrium and lateral force conditions (Fredlund 2006) can be written as follows:

$$F_m = \lim_{b_i \to 0} \frac{\sum_{i=1}^{\infty} \left\{ c'_i l_i R_i + \left[N_i - u_{w,i} l_i \frac{\tan \varphi_i^b}{\tan \varphi_i'} - u_{a,i} l_i \left(1 - \frac{\tan \varphi_i^b}{\tan \varphi_i'} \right) \right] R_i \tan \varphi_i' \right\}}{\sum_{i=1}^{\infty} W_i d_i - \sum_{i=1}^{\infty} N_i f_i}$$

$$= \lim_{b_i \to 0} \frac{\sum_{i=1}^{\infty} \left\{ c'_i \frac{b_i}{\cos \alpha_i} R_i + \left[N_i - u_{w,i} \frac{b_i}{\cos \alpha_i} \frac{\tan \varphi_i^b}{\tan \varphi_i'} - u_{a,i} \frac{b_i}{\cos \alpha_i} \left(1 - \frac{\tan \varphi_i^b}{\tan \varphi_i'} \right) \right] R_i \tan \varphi_i' \right\}}{\sum_{i=1}^{\infty} b_i \rho_i d_i - \sum_{i=1}^{\infty} \frac{N_i}{b_i} b_i f_i} \tag{1}$$

$$= \frac{\int \left\{ c' \frac{R}{\cos \alpha} + \left[\frac{dN}{dx} - \frac{u_w}{\cos \alpha} \frac{\tan \varphi^b}{\tan \varphi'} - \frac{u_a}{\cos \alpha} \left(1 - \frac{\tan \varphi^b}{\tan \varphi'} \right) \right] R \tan \varphi' \right\} dx}{\int (\rho d) dx - \int \left(\frac{dN}{dx} f \right) dx}$$

$$F_f = \lim_{b_i \to 0} \frac{\sum_{i=1}^{\infty} \left\{ c'_i l_i \cos \alpha_i + \left[N_i - u_{w,i} l_i \frac{\tan \varphi_i^b}{\tan \varphi_i'} - u_{a,i} l_i \left(1 - \frac{\tan \varphi_i^b}{\tan \varphi_i'} \right) \right] \cos \alpha_i \tan \varphi_i' \right\}}{\sum_{i=1}^{\infty} N_i \sin \alpha_i}$$

$$= \lim_{b_i \to 0} \frac{\sum_{i=1}^{\infty} \left\{ c'_i \frac{b_i}{\cos \alpha_i} \cos \alpha_i + \left[N_i \cos \alpha_i - u_{w,i} b_i \frac{\tan \varphi_i^b}{\tan \varphi_i'} - u_{a,i} b_i \left(1 - \frac{\tan \varphi_i^b}{\tan \varphi_i'} \right) \right] \tan \varphi_i' \right\}}{\sum_{i=1}^{\infty} N_i \sin \alpha_i} \tag{2}$$

$$= \frac{\int \left\{ c' + \left[\frac{dN}{dx} \cos \alpha - u_w \frac{\tan \varphi^b}{\tan \varphi'} - u_a \left(1 - \frac{\tan \varphi^b}{\tan \varphi'} \right) \right] \tan \varphi' \right\} dx}{\int \left(\frac{dN}{dx} \sin \alpha \right) dx}$$

where dx denotes width of an infinitesimal soil slice; ρ is the weight of the slice per unit width; and dN/dx is normal force at the base of the slice per unit width.

The interslice force and the normal force acting on the infinitesimally thin slice can be expressed as:

$$dN = \frac{\rho dx - dX - \frac{c'}{F_S} \tan \alpha dx + u_a \frac{\tan \alpha}{F_S} \left(\tan \varphi' - \tan \varphi^b \right) dx + u_w \frac{\tan \varphi^b}{F_S} \tan \alpha dx}{m_\alpha} \tag{3}$$

$$dX = \lambda f(x) dE \tag{4}$$

$$dE = (\rho \tan \alpha) dx - \tan \alpha dX - \frac{1}{\cos \alpha} dS_m \tag{5}$$

where,

$$dS_m = \frac{1}{F_s} \left\{ \frac{c'}{\cos \alpha} dx + \tan \varphi' dN + \left[\frac{u_a}{\cos \alpha} \left(\tan \varphi^b - \tan \varphi' \right) - \frac{u_w}{\cos \alpha} \tan \varphi^b \right] dx \right\} \tag{6}$$

Only four unknown variables, including dN, dX, dE, and dS_m, within the above linear equation group. Thus,

by rearranging Eqs. (11) to (14), *dN* can be obtained as:

$$dN = \frac{1}{\bar{m}_\alpha}\left[\rho - \frac{c'}{F_S}\tan\alpha + u_a\frac{\tan\alpha}{F_S}\left(\tan\varphi' - \tan\varphi^b\right) + u_w\frac{\tan\alpha}{F_S}\tan\varphi^b\right]dx + \frac{1}{\bar{m}_\alpha\lambda f(x)F_S}\left[c' + u_a\left(\tan\varphi^b - \tan\varphi'\right) - u_w\tan\varphi^b\right]dx \tag{7}$$

where,

$$\bar{m}_\alpha = m_\alpha + \lambda f(x)\left(\sin\alpha - \cos\alpha\frac{\tan\varphi'}{F_S}\right) \tag{8}$$

But even the expression of *dN* is obtained, the analytical solutions for Eqs. (1) and (2) are still hard to be derived. Thus, a numerical integral technique, named the Gaussian integral, is introduced for simplifying the expression of FOSs. Using the Gaussian integral, Eqs. (1) and (2) can be rewritten as:

$$F_m = \frac{\sum_{j=1}^{NG}\omega_j\left\{c_j'\frac{R_j}{\cos\alpha_j} + \left[\overline{N}_j - \frac{u_{w,j}}{\cos\alpha_j}\frac{\tan\varphi_j^b}{\tan\varphi_j'} - \frac{1}{\cos\alpha_j}u_{a,j}\left(1 - \frac{\tan\varphi_j^b}{\tan\varphi_j'}\right)\right]R_j\tan\varphi_j'\right\}}{\sum_{j=1}^{NG}\omega_j\left(\rho_j d_j\right) - \sum_{j=1}^{NG}\omega_j\left(\overline{N}_j f_j\right)} \tag{9}$$

$$F_f = \frac{\sum_{j=1}^{NG}\omega_j\left\{c_j' + \left[\overline{N}_j\cos\alpha_j - u_{w,j}\frac{\tan\varphi_j^b}{\tan\varphi_j'} - u_{a,j}\left(1 - \frac{\tan\varphi_j^b}{\tan\varphi_j'}\right)\right]\tan\varphi_j'\right\}}{\sum_{j=1}^{NG}\omega_j\left(\overline{N}_j\sin\alpha_j\right)} \tag{10}$$

where,

$$\overline{N} = \frac{1}{\bar{m}_\alpha}\left[\rho - \frac{c'}{F_S}\tan\alpha + u_a\frac{\tan\alpha}{F_S}\left(\tan\varphi' - \tan\varphi^b\right) + u_w\frac{\tan\alpha}{F_S}\tan\varphi^b\right] + \frac{1}{\bar{m}_\alpha\lambda f(x)F_S}\left[c' + u_a\left(\tan\varphi^b - \tan\varphi'\right) - u_w\tan\varphi^b\right] \tag{11}$$

in which, *NG* is the number of Gauss points; the subscript $_j$ denotes the number of Gauss point; and ω is the weight coefficient of Gauss point.

To maintain the function's continuity within the domain, the slip surface should be divided into several integration intervals when the present study is employed for some slip surfaces with gradient-discontinuity points or passing through interfaces of soil layers. Therefore, the FOS expressions can be further rewritten for generality as:

$$F_m = \frac{\sum_{k=1}^{NI}\left(x^k - x^{k-1}\right)\sum_{j=1}^{NG}\omega_{kj}\left\{c_{kj}'\frac{R_{kj}}{\cos\alpha_{kj}} + \left[\overline{N}_{kj} - \frac{u_{w,kj}}{\cos\alpha_{kj}}\frac{\tan\varphi_{kj}^b}{\tan\varphi_{kj}'} - \frac{1}{\cos\alpha_{kj}}u_{a,kj}\left(1 - \frac{\tan\varphi_{kj}^b}{\tan\varphi_{kj}'}\right)\right]R_{kj}\tan\varphi_{kj}'\right\}}{\sum_{k=1}^{NI}\left(x^k - x^{k-1}\right)\sum_{j=1}^{NG}\omega_{kj}\left(\rho_{kj}d_{kj}\right) - \sum_{k=1}^{NI}\left(x^k - x^{k-1}\right)\sum_{j=1}^{NG}\omega_{kj}\left(\overline{N}_{kj}f_{kj}\right)} \tag{12}$$

$$F_f = \frac{\sum_{k=1}^{NI}\left(x^k - x^{k-1}\right)\sum_{j=1}^{NG}\omega_{kj}\left\{c_{kj}' + \left[\overline{N}_{kj}\cos\alpha_{kj} - u_{w,kj}\frac{\tan\varphi_{kj}^b}{\tan\varphi_{kj}'} - u_{a,kj}\left(1 - \frac{\tan\varphi_{kj}^b}{\tan\varphi_{kj}'}\right)\right]\tan\varphi_{kj}'\right\}}{\sum_{k=1}^{NI}\left(x^k - x^{k-1}\right)\sum_{j=1}^{NG}\omega_{kj}\left(\overline{N}_{kj}\sin\alpha_{kj}\right)} \quad (13)$$

where NI denotes the number of intervals of integration; the subscript k is the number of the interval of integration; and x^{k-1} and x^k are two end points of the interval of integration, which should be the intersection point between the slip surface or the gradient-discontinuity point of the slip surface (as demonstrated in Fig. 2).

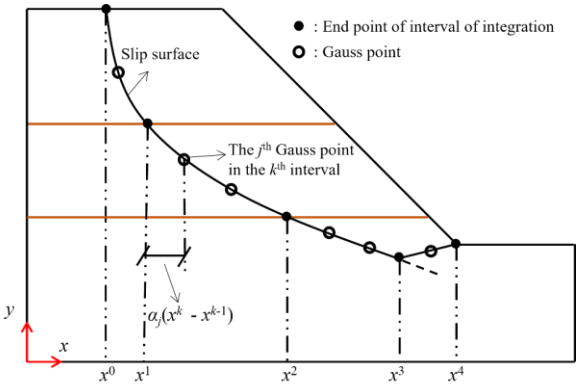

Figure 2: Alignment of Gauss points in the proposed method

The location of the adopted Gauss point, (x_{kj}, y_{ky}), can be calculated as follows:

$$x_{kj} = \alpha_j(x^k - x^{k-1}) + x^{k-1} \quad (14)$$

$$y_{kj} = S(x_{kj}) \quad (15)$$

where α is the dimensionless coefficient of Gauss point; and $S(x)$ is the shape function of the slip surface. It is recommended to use 3-5 Gauss points in one integral region to achieve reliable results. More Gauss points can also be defined based on the specific situation.

2.2 Refined procedures for solving FOS

The solving procedures for the FOS in the present study include two parts: (1) solving the FOS with the selected scaling factor; (2) obtaining the scaling factor satisfying the total equilibrium conditions.

When solving factor of safety equations in the traditional MP method, the interslice force distribution must be assumed to be zero initially. Then, in each iterative step, the interslice force should be updated separately, leading to a tedious computational procedure. In the present study, a set of more concise iteration procedures (see Fig. 3) can be described as follows:

(i) Input slope conditions and λ.
(ii) Align Gauss points.
(iii) Set $F_{s,i} = 1.0$.
(iv) Get the normal force at each Gauss point.
(v) Calculate $F_{s,i+1}$ according to Eq. (12) or Eq.(13).
(vi) Set $F_{s,i} = F_{s,i+1}$ and return to Step (iv) until the differences in values of F_s between two consecutive iterations are within specified limits of tolerance, TOL.

It is convenient to implement the best-fit regression method for searching the scaling factor for the total equilibrium condition. However, the data points must be distributed densely enough to searching the accurate results of the joining between F_m and F_f, implying the relatively large computational effort is taken in the analysis. For efficiently searching the scaling factor satisfying both moment and force equilibrium conditions, a linear searching method is employed in the present study. The linear searching method (as illustrated in Fig. 4) can be described as follows:

Proceedings DOI: 10.21467/proceedings.7.7
ISBN: 978-81-989164-3-3

Series: AIJR Proceedings
ISSN: 2582-3922

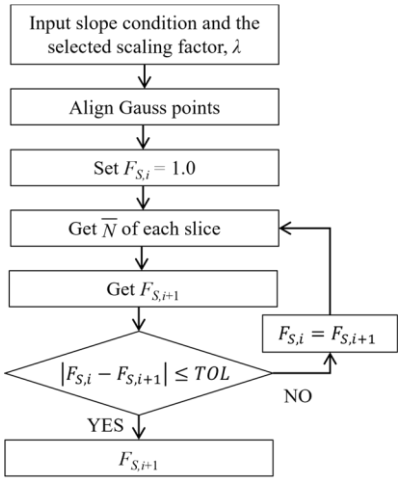

Figure 3: Solving FOS with the selected scaling factor in the present study

(i) Input the searching range [λ_L, λ_R].
(ii) Obtain $\Delta F(\lambda_L)$ and $\Delta F(\lambda_R)$, where $\Delta F(\lambda) = F_m(\lambda) - F_f(\lambda)$.
(iii) Calculate λ_M using the secant relation as:

$$\lambda_M = \frac{\lambda_L \Delta F(\lambda_R) + \lambda_R \Delta F(\lambda_L)}{\Delta F(\lambda_R) - \Delta F(\lambda_L)}$$

(iv) Check whether $\Delta F(\lambda_M)$ achieves the convergence criterion. If the convergence tolerance is satisfied, output λ_M as the result. Otherwise, return to Step (iv) and update the searching range according to:

$$\lambda_L = \begin{cases} \lambda_L & if \quad \Delta F(\lambda_L)\Delta F(\lambda_M) < 0 \\ \lambda_M & if \quad \Delta F(\lambda_L)\Delta F(\lambda_M) \geq 0 \end{cases} \quad AND \quad \lambda_R = \begin{cases} \lambda_R & if \quad \Delta F(\lambda_R)\Delta F(\lambda_M) < 0 \\ \lambda_M & if \quad \Delta F(\lambda_R)\Delta F(\lambda_M) \geq 0 \end{cases}$$

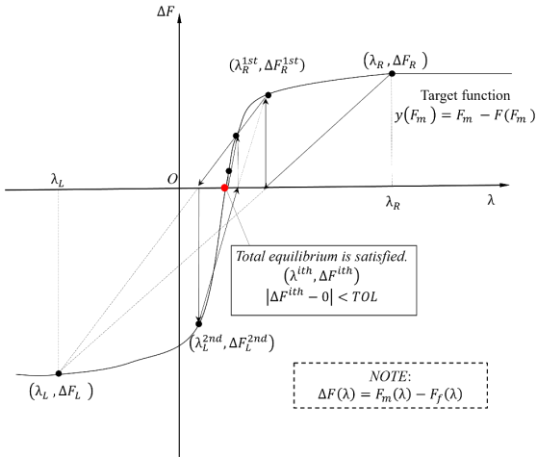

Figure 4: Schematic diagram of linear search algorithm for determining the scaling factor

3 VERIFICATION EXAMPLES

In this section, two typical types of slopes are studied to validate the present method based on Gaussian integral for assessing the stability of unsaturated soil slopes, including homogeneous and nonhomogeneous slopes.

3.1 Example 1: Stability analysis of a homogeneous unsaturated soil slope

In this example, a steep and homogeneous slope with a height of 30 m and a slope angle of 50° is re-analysed (Zhang et al. 2014). Fig. 5 illustrates the geometry of this homogenous steep slope and prescribed critical slip surface. The unit weight of the soil is γ = 18 kN/m^3. The cohesion and effective internal friction angle of the soil are c' = 10 kPa and φ' = 34°, respectively. The average depth of piezometric line is more than 10 m below the surface of slope.

A specific slip surface is selected for evaluating the stability of this unsaturated soil slope (see Fig. 5). Table 1 lists the values of FOS of the slope with the prescribed slip surface under different φ^b-values. The FOS-values of the unsaturated soil slope in this study are generally consistent with those calculated by Zhang et al. (2014). The FOS of slope increases gradually with the increase of φ^b. This increasing trend is because the increasing φ^b has enhanced the shear strength listed in Eq. (1), and thus, the enhancing mobilized shear force shown in Eq. (8) at the slice base increases. The error is also evaluated, which is defined by ratio of difference between the previous value of FOS and FOS in the present study to the FOS in the present study. The error decreases with the increasing φ^b.

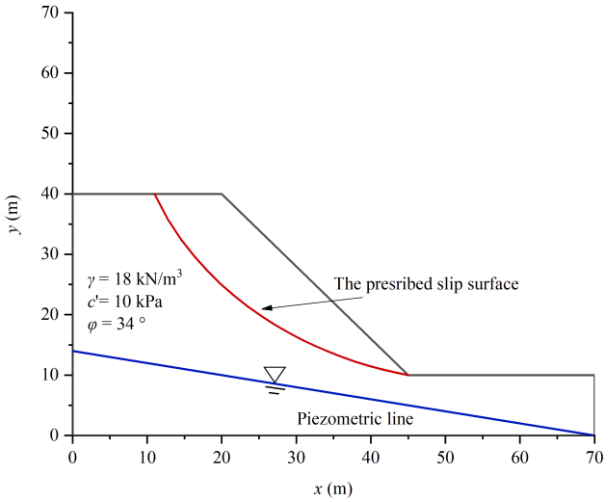

Figure 5: Geometry and prescribed critical slip surface of a homogenous unsaturated soil slope

Table 1: FOS under different values of φb for the example of a homogenous unsaturated soil slope

φ^b (°)	FOS in Zhang et al. (2014)	FOS in present study	Error
0	1.005	1.001	0.39 %
15°	1.430	1.426	0.28 %
34°	2.118	2.121	0.14 %

The traditional MP method has also been used to validate the new method. The numbers of soil slices for traditional MP method and gauss points for present study are 32 and 5, respectively. Table 2 summarises the FOS and computational cost in the present proposed and traditional MP methods for this example. The improved MP method using Gaussian integral with only 5 Gauss points shows much higher efficiency than the traditional MP method with 32 slices, no matter which value of φ^b is assumed. In general, for different values of φ^b, the time used in the present study is approximately only one tenth of that used in the traditional MP method. Fig. 6 shows comparisons of critical slip surfaces based on the present study and traditional MP method for the homogenous slope. The critical slip surfaces obtained from the present study agree well with those surfaces suggested by Zhang et al. (2014) . The depth of critical slip surface increases with the rising φ^b. Compared with the other two critical slip surfaces, the critical slip surface for $\varphi^b = \varphi'$ is much deeper. This example demonstrates the accuracy and efficiency of this improved MP method in evaluating the stability of unsaturated and homogenous soil slope. In addition, Table 2 also demonstrates that ignoring unsaturated characteristic of soil by taking $\varphi^b = 0°$ will lead to significant underestimation of slope stability, underscoring the critical need to accurately account for the unsaturated properties of soil in slope stability assessment.

Table 2: FOS and computational cost in different methods for the example of a homogenous slope

Analysis method	n_{SP}	φ^b (°)	FOS	Computational time (s)
Traditional MP	32 slices	0	0.887	1202
		15	1.420	1532
		34	1.908	1598
Present study	5 Gauss points	0	0.895	113
		15	1.399	122
		34	1.879	185

Proceedings DOI: 10.21467/proceedings.7.7
ISBN: 978-81-989164-3-3

Series: AIJR Proceedings
ISSN: 2582-3922

Notes: n_{SP} denotes the number of sampling points in different methods

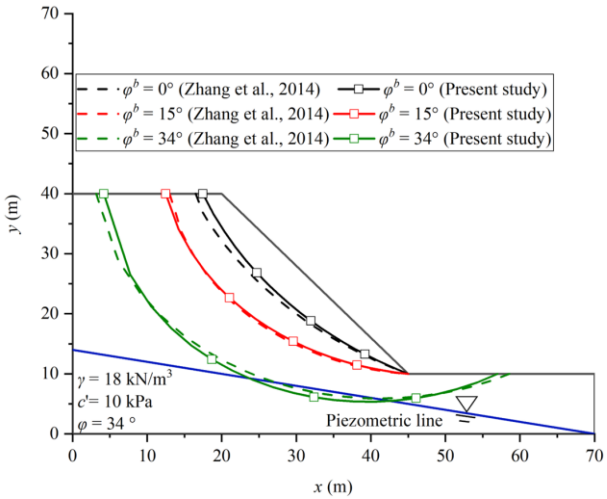

Figure 6: Critical slip surfaces based on present study and traditional MP method for a homogenous unsaturated soil slope

3.2 Example 2: Stability analysis of a nonhomogeneous unsaturated soil slope

Example 2 was originally presented by Fredlund et al. (2006). The example is a nonhomogeneous slope with three layers, in which there is a weak layer between medium and hard layers. The geometry, soil properties of different layers, and piezometric line are shown in Fig. 7. Fredlund et al. (2006) compared the values of FOS based on dynamic programming method and MP method and found that FOS of dynamic programming method was around 14% lower than that of MP method. The critical slip surface is highly irregular and influenced by the position of weak layer.

Here, the example is reanalysed using the proposed method and traditional MP method. In this example, 3-4 Gauss points are aligned at each soil layer in the proposed method. The different values of FOS for different values of φ^b based on these two methods are shown in Fig. 7. In general, with the rise of φ^b, the critical slip surface gets shallower for the two methods. The shape of critical slip surfaces changes from a typical circular arc to an irregular shape. It seems that the position of weak layer affects the shape of critical slip surfaces and leads to the irregular shape of critical slip surfaces. This phenomenon agrees well with those observed by Fredlund et al. (2006). For both two methods, the FOS decreases with the increase of φ^b. The declining trend of FOS with increasing φ^b for the nonhomogeneous slope is different from the increasing trend observed in a homogeneous slope since the FOS is influenced by the combination of factors, such as soil layers, soil properties, and piezometric line. The FOS results based on proposed method are generally consistent with those based on the traditional MP method. This example shows the effectiveness and accuracy of this proposed method in evaluation of stability of nonhomogeneous slope.

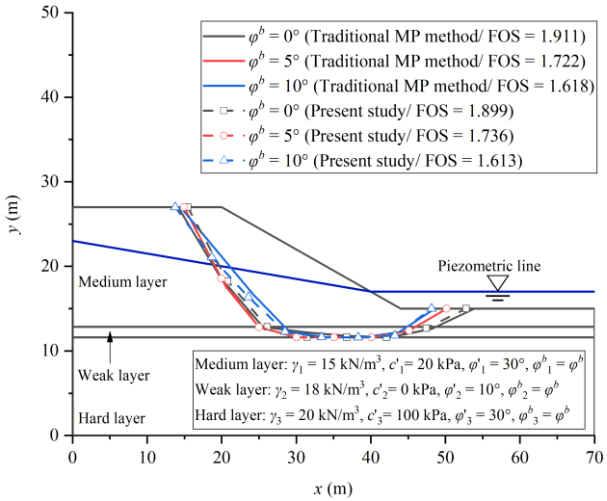

Figure 7: Critical slip surfaces based on present study and traditional MP method for a nonhomogeneous unsaturated soil slope

4 CASE STUDY: STABILITY ANALYSIS OF A CUT SLOPE OF WEATHERED GRANITE

As shown in Fig. 8, a steep cut slope of weathered granite behind a hospital and residential buildings in Hong Kong is investigated. There have been dangerous small periodic failures at the crest of slope, which require a comprehensive investigation. The average inclination of the slope is 60°. The slope surface is a layer of soil cement and lime plaster which can protects the slope from water infiltration. The soil stratigraphy is broadly distributed in Hong Kong especially for the colluvial slopes in the mountain area, including granitic colluvium, completely weathered granite, and highly weathered granite. The weathered granite is one of the most common residual soils in Hong Kong. The depth of bedrock is 20 to 30m below the ground surface. The approximate position of water table is located in the bedrock. Table 3 lists the soil properties of different layers in the case study. The average value of φ^b is 15.0° based on the results of triaxial tests (Ho & Fredlund 1982). The measured soil suction ranges from approximately 0 to 80 kPa due to different elevations. With the increasing elevation, the soil suction gets greater.

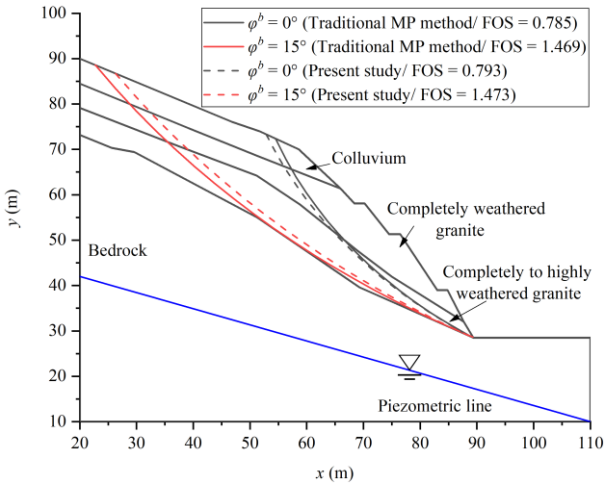

Figure 8: Critical slip surfaces based on present study and traditional MP method for an unsaturated soil slope of weathered granite

Table 3: Soil properties in the case study

Soil type	γ (kN/m^3)	c' (kPa)	φ' (°)	φ^b (°)
Colluvium	19.6	10.0	35.0	15.0
Completely weathered granite	19.6	15.1	35.2	15.0
Completely to highly weathered granite	19.6	23.5	41.5	15.0

This case study has been re-analysed by comparing the slope-stability evaluation using the efficient LEM based on Gaussian integral and the traditional MP method (see Fig. 8). 3-4 Gauss points are placed in each soil layer in this case study. In the analysis, the suction was ignored (φ^b = 0°) firstly. The FOS-values based on the traditional MP method and present method are 0.785 and 0.793, respectively. These results can generally agree well with the FOS of 0.864 based on the Bishop simplified method. These slight differences might be due to the different assumptions in these methods, such as different force equilibrium conditions and soil discretization methods, etc. Nevertheless, it seems that the slope is still stable. This might be attributed to the enhanced shearing strength due to suction has strengthened the slope stability, reflecting the significant role of suction in soil slope stability. Secondly, the average value of φ^b which is equal to 15.0° was adopted in the analysis. The values of FOS for the traditional MP method and present method are 1.469 and 1.473, respectively. It shows that the consideration of suction has greatly enhanced the slope stability. In addition, the critical slip surfaces based on these two methods are consistent with each other no matter whether the suction is considered or not. With the increase of φ^b, the depth of critical slip surface gets deeper. These results of FOS-values and critical slip surfaces agree well with those observed by Zhang et al. (2014). Moreover, the

Proceedings DOI: 10.21467/proceedings.7.7
ISBN: 978-81-989164-3-3

Series: AIJR Proceedings
ISSN: 2582-3922

computational cost with different methods on the same device are also given in Table 4 to illustrate the computational efficiency of the proposed method.

Table 4: Computational cost of different methods in case study

Analysis method	Average computational time
Traditional MP method	15 min
Present study	3 min

5 CONCLUSIONS

This study presents an efficient numerical implementation of limit equilibrium method (LEM) based on the Morgenstern-Price method using Gaussian integral for stability analysis of unsaturated soil slopes. This new method is an extension of the improved Morgenstern-Price method proposed by Ouyang et al. (2022). Compared with the other methods, this method may be a useful attempt and might provide a new solution to evaluate the stability of unsaturated soil slopes. Conclusions are mainly summarized as follows:

(1) The extended Mohr–Coulomb shear strength equation is adopted to be the governing shearing strength equation in the analysis of slope stability. In traditional LEM, the slice division shall be dense enough by increasing the slice number to achieve reliable results. However, in the new method, a numerical integral technique named Gaussian integral, is introduced for simplifying the expressions and calculations of FOS values. In addition, the solving procedures for the FOS in the present study mainly include two parts, including solving the FOS with the selected scaling factor and determining the scaling factor satisfying the total equilibrium conditions. Based on the developed formula, the iteration process for calculating the FOS with the given scaling factor is refined where the step of assuming the initial force distribution is eliminated. Besides, the linear search method is used in searching the scaling factor to fulfil the total equilibrium conditions.

(2) This new method is validated based on two typical benchmark examples such as homogeneous and nonhomogeneous unsaturated soil slopes and one case study of unsaturated residual soil slope in Hong Kong. Overall, compared with the traditional MP method, the newly proposed method with a few Gauss points is reliable, accurate, and efficient in evaluating the stability of unsaturated soil slopes.

ACKNOWLEDGEMENTS

The Start-up Fund for RAPs under the Strategic Hiring Scheme from PolyU (UGC) (Project ID: P0045938) is acknowledged. The authors also acknowledge the supports by a RIF project (Grant No.: R5037-18) and GRF projects (Grant No.: 15217918, 15213019, 15210020, 15231122) from Research Grants Council (RGC) of Hong Kong Special Administrative Region Government of China. The authors also acknowledge the financial support from grants (CD7A and CD82) from the Research Institute for Land and Space of Hong Kong Polytechnic University, and financial support (W23L, ZDBS) from The Hong Kong Polytechnic University. This financial support is gratefully acknowledged. This work is also partially supported by grants from the Research Grants Council of the Hong Kong Special Administrative Regain, China (Grant No.: 15203121).

REFERENCES

Cai, F., Ugai, K. 2004. Numerical analysis of rainfall effects on slope stability. *Int J Geomech*, 4(2): 69–78.

Xiong, X., Shi, Z., Xiong, Y., Peng, M., Ma, X. & Zhang, F. 2019. Unsaturated slope stability around the Three Gorges Reservoir under various combinations of rainfall and water level fluctuation. *Eng Geol*, 261(December 2018): 105231.

Houston, S.L. 2019. It is time to use unsaturated soil mechanics in routine geotechnical engineering practice. *J Geotech Geoenviron Eng*, 145(5): 02519001.

Sun, D., Wang, L., Li, L. 2019. Stability of unsaturated soil slopes with cracks under steady-infiltration conditions. *Int J Geomech*, 19(6): 04019044.

Griffiths, D.V., Lu, N. 2005. Unsaturated slope stability analysis with steady infiltration or evaporation using elasto-plastic finite elements. *Int J Numer Anal Methods Geomech*, 29(3): 249–267.

Duncan, M.J. 1996. State of the art: limit equilibrium and finite- element analysis of slopes. *J Geotech Eng*, 122(7): 577–596.

Ouyang, W., Liu, S.W., Yang, Y. 2022. An improved morgenstern- price method using gaussian quadrature. *Comput Geotech*, 148: 104754.

Cheng, Y.M., Lau, C. 2014. Slope stability analysis and stabiliza- tion: new methods and insight. CRC Press, Boca Raton.

Fredlund, D.G., Morgenstern NR, Widger RA 1978. The shear strength of unsaturated soils. *Can Geotech J*, 15(3): 313–321

Fredlund, D.G. 2006. Unsaturated soil mechanics in engineering practice. *J Geotech Geoenviron Eng*, 132(3): 286–321.

Zhang, L.L., Fredlund, D.G., Fredlund, M.D., Ward, Wilson G. 2014. Modeling the unsaturated soil zone in slope stability analysis. *Can Geotech J*, 51(12): 1384–1398.

Ho, D.Y., Fredlund, D.G. 1982. Increase in strength due to suction for two Hong Kong soils. *Proceedings of the ASCE specialty conference on engineering and construction in tropical and residual soils*, Hawaii. p. 263-96.

Proceedings DOI: 10.21467/proceedings.7.7
ISBN: 978-81-989164-3-3

Series: AIJR Proceedings
ISSN: 2582-3922